

# POST-TRAINING QUANTIZATION FOR CROSS-PLATFORM LEARNED IMAGE COMPRESSION

Dailan He, Ziming Yang\*, Yuan Chen\*, Qi Zhang, Hongwei Qin

SenseTime Research

{hedailan, yangziming, chenyan1, zhangqi3, qinhongwei}@sensetime.com

Yan Wang<sup>†</sup>

SenseTime Research

Tsinghua University

wangyan1@sensetime.com, wangyan@air.tsinghua.edu.cn

## ABSTRACT

It has been witnessed that learned image compression has outperformed conventional image coding techniques and tends to be practical in industrial applications. One of the most critical issues that need to be considered is the non-deterministic calculation, which makes the probability prediction cross-platform inconsistent and frustrates successful decoding. We propose to solve this problem by introducing well-developed post-training quantization and making the model inference integer-arithmetic-only, which is much simpler than presently existing training and fine-tuning based approaches yet still keeps the superior rate-distortion performance of learned image compression. Based on that, we further improve the discretization of the entropy parameters and extend the deterministic inference to fit Gaussian mixture models. With our proposed methods, the current state-of-the-art image compression models can infer in a cross-platform consistent manner, which makes the further development and practice of learned image compression more promising.

## 1 INTRODUCTION



(a) original image

(b) failed decoding

Figure 1: The cross-platform inconsistency caused by non-deterministic model inference. This inconsistency is a catastrophe to establish general-purpose image compression systems, and it is almost inevitable when practicing learned image compression with floating-point arithmetic.

In recent years, learned data compression techniques have attracted a lot of attention and achieved remarkable progress (Ballé et al., 2017; 2018; Minnen et al., 2018; Cheng et al., 2020; He et al.,

\*This work is done when Ziming Yang and Yuan Chen are interns at SenseTime Research.

<sup>†</sup>Corresponding author.

---

2021; Guo et al., 2021). Recently, a few learned lossy image compression approaches (Minnen et al., 2018; Cheng et al., 2020; He et al., 2021; Guo et al., 2021) have outperformed BPG (Bellard, 2015) and the intra-frame coding of VVC (vtm, 2020), which are the state-of-the-art manually designed image compression algorithms. As lossy image compression is one of the most fundamental techniques of visual data encoding, these results promise possibility of transmitting and storing images or frames at a lower bit rate, which can benefit almost all industrial applications dealing with visual data. Therefore, it is highly important to study how to make these rapidly developing learning-based methods practical.

Most currently state-of-the-art learned image compression approaches adopt a forward-adaptive coding scheme proposed in Ballé et al. (2018). The model will firstly transform the image to a major representation  $\hat{y}$  and a minor representation  $\hat{z}$ . Then  $\hat{y}$  will be encoded by an arithmetic coder (Rissanen & Langdon, 1981; Martin, 1979) with independently saved  $\hat{z}$  as side-information. Later this method is further delved by introducing backward adaption with context modeling (Minnen et al., 2018; He et al., 2021; Guo et al., 2021). However, this line of models suffer from a non-determinism issue (Ballé et al., 2019), which makes the image hard to be decoded when the encoder and the decoder run on heterogeneous platforms. The non-determinism is caused by floating-point arithmetic, which can let the calculation results, from the same input operands but on different software or hardware platforms, different. This issue makes calculating prior from side-information and context model cross-platform inconsistent so that the decoding fails (See Figure 1). As cross-platform transmission is a vital requirement of establishing practical image coding systems, this inconsistency is critical.

To make the computation deterministic for cross-platform consistency, Ballé et al. (2019) proposes to train an integer network specially designed for learned image compression, where the inference stage is integer-arithmetic-only. It performs well on earlier proposed models like Ballé et al. (2018). After determinizing Ballé et al. (2018) with integer network, the compression performance has a marginal reduction compared with the floating-point version. However, we find that on more complex models with context modeling like Minnen et al. (2018) and Cheng et al. (2020), adopting this integer network approach cannot keep the performance loss negligible. Another previous work (Sun et al. (2021)) proposes to quantize model parameters and activation to fix-point, enabling cross-platform decoding of the mean-scale hyperprior-only network in Minnen et al. (2018) without hurting compression performance. However, the determinism of state-of-the-art joint autoregressive and hyperprior methods (Minnen et al., 2018; Cheng et al., 2020; He et al., 2021; Guo et al., 2021) are still not considered. As the slow serial decoding problem of autoregressive context model has been addressed in He et al. (2021), this joint modeling architecture is very promising and valuable for practical application and its cross-platform decoding issue needs to be solved.

We notice that, these existing approaches are similar to general model quantization techniques in spirit, *i.e.* quantization-aware training (QAT, Jacob et al. (2018); Krishnamoorthi (2018); Esser et al. (2019); Bhalgat et al. (2020)) and post-training quantization (PTQ, Nagel et al. (2019; 2020); Li et al. (2020)). Instead of proposing another approach to provide an ad-hoc solution, we advocate to solve this cross-platform consistency issue based on those well-developed model quantization techniques in a more flexible and extendable manner. Thus, we investigate cross-platform consistent inference with PTQ. Usually, it requires much less calibration data (Nagel et al., 2020; 2021; Li et al., 2020) and costs much less time to quantize the model than QAT, yet for several computer vision tasks it can achieve almost the same accuracy as QAT when the target bit-width is 8 (Nagel et al., 2019; 2020; Li et al., 2020). It does not demand re-training or fine-tuning the trained floating-point models, which is very friendly to industrial deployment. By applying integer-arithmetic-only operators (Jacob et al., 2018; Zhao et al., 2020; Yao et al., 2021) after quantization, we can achieve deterministic models which get rid of the inconsistency issue.

In this paper, we contribute to the community from following perspectives:

1. We evaluate and prove that, the deterministic computing issue of learned data compression can be reduced to a general model quantization problem. After applying a standard post-training quantization (PTQ) technique, we obtain cross-platform consistent image compression models with marginal compression performance loss.
2. We successfully determinize presently state-of-the-art learned image compression models with context modeling and Gaussian mixture models. To the best of our knowledge, this is the first work investigating and accessing cross-platform consistent inference on those

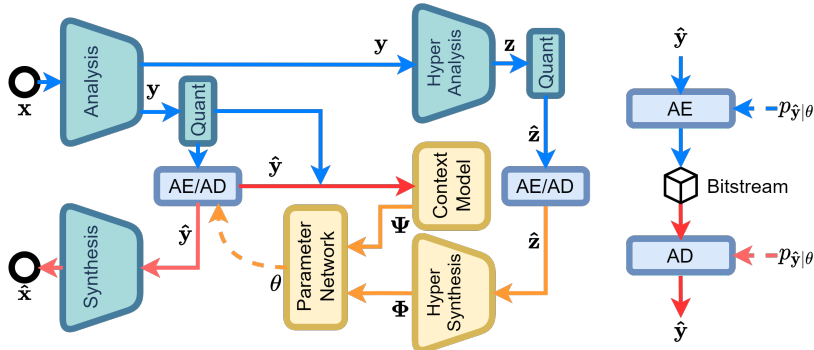


Figure 2: Diagram of joint autoregressive and hyperprior architecture for learned image compression (Minnen et al., 2018; Cheng et al., 2020). AE/AD denote arithmetic en/de-coder.  $\theta$  is the set of predicted entropy parameters (*i.e.*  $\pi, \mu, \sigma$ ), modeling the distribution of  $\hat{y}$  element-wisely. The blue, red and orange arrows denote encoding, decoding and shared data flows, respectively. The highlighted orange networks are shared by both encoding and decoding to estimate code probability for AE/AD, demanding cross-platform consistency.

models. As we use standard quantization techniques, it is also promising to adopt our method to determinize future compression models.

3. We propose a novel approach to discretize the entropy parameters, which can be computed directly in a deterministic manner. Compared with the existing method based on searching algorithm, our method significantly speeds up the parameter discretization and eliminates the bottleneck.

We emphasize that our goal is not to propose a new method for quantizing neural networks, but to call attention to the relation between the deterministic issue and model quantization techniques. Benefiting from the maturely developed quantization techniques, we show that the cross-platform consistency issue in learned image compression can be better solved.

## 2 PRELIMINARY

### Notations.

We represent matrices with capital bold letters (*e.g.*  $\mathbf{W}$ ) and denote vectors as small bold letters (*e.g.*  $\mathbf{v}$ ). We use ceiling  $\lceil \cdot \rceil$  and floor  $\lfloor \cdot \rfloor$  notations to represent round-up and round-down operators, respectively. And the blended  $\lceil \cdot \rceil$  denotes round-to-nearest. By default, we denote the inputs and activated outputs of a linear layer as  $\mathbf{v}$  and  $\mathbf{u}$  respectively. And the activation function is represented by  $h(\cdot)$ . We use the capital  $B$  as the quantization bit-width, which by default is set to 8 as we prefer an 8-bit quantization. We use scalar  $s$  with a subscript to denote the corresponding quantization step, *e.g.*  $s_{\mathbf{v}}$  means the quantization step of  $\mathbf{v}$ . We may introduce a bracketed superscript to distinguish variables in different layers, *e.g.*  $\mathbf{v}^{(\ell)}$  is the input of the  $\ell$ -th layer while  $\mathbf{v}^{(\ell+1)}$  is the input of the next layer. For simplicity, we use the notation  $\text{clip}(\cdot)$  as value clipping introduced by uniform affine quantization, omitting the clipping bounds. By default we quantize the tensors to  $B$ -bit signed integers, with the upper and lower clipping bounds  $2^{B-1} - 1$  and  $-2^{B-1}$ .

**Learned image compression and non-determinism issue.** Briefly speaking, almost all the cutting-edge learned image compression techniques adopt the joint autoregressive and hyperprior modeling illustrated in Figure 2. To encode the major symbols  $\hat{y}_i$ , an entropy model  $p_{\hat{y}_i | \hat{\mathbf{z}}, \hat{\mathbf{y}}_{j < i}}(\hat{y}_i; \hat{\mathbf{z}}, \hat{\mathbf{y}}_{j < i})$  is adopted to predict the probability density of  $\hat{y}_i$  conditioned on side-information  $\hat{\mathbf{z}}$  and already decoded symbols  $\hat{\mathbf{y}}_{j < i}$ . The predicted density functions will then be accumulated to obtain the cumulative distribution functions (CDF) and fed to arithmetic en/de-coders.

Generally, we input  $\hat{\mathbf{z}}$  to the *hyper synthesizer* to obtain the intermediate feature  $\Phi$ , and use the *context models* to summarize the context representation  $\Psi$ . Then, we use a *parameter network* to calculate the element-wise distribution parameters from  $\Phi$  and  $\Psi$  to generate the predicted distri-

butions. To ensure correct decompression, we should make sure the inference of above-mentioned models (*hyper synthesizer*, *context models* and *parameter network*) *deterministic*. It means that, with the same input  $\hat{\mathbf{z}}$  and  $\hat{\mathbf{y}}_{j < i}$ , the predicted entropy parameters  $\theta$  should always be the same no matter what platform the encoder or decoder is running on. The calculation should be platform-independent and cross-platform consistent. However, if the models infer with floating-point numbers, the determinism is hard to satisfy.

**Uniform affine quantization (UAQ).** UAQ is widely adopted by model quantization researches (Jacob et al., 2018; Nagel et al., 2019; 2020; Li et al., 2020). In UAQ, both activation values and weights should be quantized to fixed point numbers to allow the use of integer matrix multiplications. Usually, UAQ maps floating-point values to  $B$ -bit integers. For a given vector  $\mathbf{v}$ , UAQ with a quantization step  $s_v$  is formulated as:

$$\mathbf{q}_v = \text{clip} \left( \lceil s_v^{-1} \mathbf{v} \rceil + z_v \right) \quad (1)$$

The term  $z_v$  is an integer representing the zero-point shifting the center of quantization range, which is applied in asymmetric uniform affine quantization and omitted in symmetric ones. In recent QAT, the step  $s_v$  and zero-point  $z_v$  are usually learned during training/fine-tuning (Esser et al., 2019). And in PTQ they are normally determined by the value range of given weights or activation vectors (Nagel et al., 2019; 2021).

Therefore, the floating point vector  $\mathbf{v}$  is discretized to an integer vector  $\mathbf{q}_v$ , where each integer value actually represents a fixed point value. We can remap  $\mathbf{q}_v$  to corresponding fix-point vector through dequantization:

$$\hat{\mathbf{v}} = s_v \mathbf{q}_v - s_v z_v \quad (2)$$

When  $\mathbf{v}$  is the activation output, the second term can be pre-computed and absorbed by the convolution bias, so it will not introduce extra calculation to inference. Therefore, it is recommended by Nagel et al. (2021) to apply asymmetric quantization on activation and symmetric quantization on weights. Nagel et al. (2021) also suggests to adopt a per-channel quantization on weights (Krishnamoorthi, 2018; Li et al., 2019).

**Integer-arithmetic-only requantization.** Several previous works on QAT for integer-arithmetic-only inference have been proposed (Jacob et al., 2018; Zhao et al., 2020; Yao et al., 2021). One of the most important techniques is the dyadic requantization. Between two convolution layers, the dequantized fixed point activation will get quantized again, this can be fused to one operation called requantization. A requantization after the  $\ell$ -th layer is:

$$\mathbf{q}_v^{(\ell+1)} = \text{clip} \left( \lceil m^{(\ell)} \mathbf{q}_u^{(\ell)} \rceil + z_u^{(\ell)} \right) \quad (3)$$

where  $\mathbf{q}_u^{(\ell)}$  is the int32 activation accumulation of the  $\ell$ -th layer,  $z_u^{(\ell)}$  is the zero point, and  $m^{(\ell)}$  is the requantization scale factor.

Ideally, all floating-point operator should be removed from model inference but  $m$  is still floating-point, which makes the requantization non-deterministic. Therefore, a dyadic number  $m_0$  is introduced in Jacob et al. (2018) to approximate  $m$ :

$$m_0 = \lceil 2^n m \rceil \quad (4)$$

where  $m_0$  and  $n$  are integers. Now we have  $m \approx 2^{-n} m_0$ . Obviously, the approximation error becomes smaller when  $n$  gets larger. With this approximation, the requantization described in eq. 3 can be rewritten as:

$$\mathbf{q}_v^{(\ell+1)} = \text{clip} \left( \left\lceil \frac{m_0^{(\ell)} \mathbf{q}_u^{(\ell)}}{2^{n^{(\ell)}}} \right\rceil + z_u^{(\ell)} \right) = \text{clip} \left( \left\lceil \left( m_0^{(\ell)} \mathbf{q}_u^{(\ell)} \right) // 2^{n^{(\ell)}} \right\rceil + z_u^{(\ell)} \right) \quad (5)$$

where the operator  $//$  is integer division with rounding-to-nearest (round-int-div, RID). And this RID calculation can be further implemented as bit shift operation with rounding-to-nearest (round-int-shift, RIS). Since both  $m_0$  and 32-bit activation  $\mathbf{q}_u^{(\ell)}$  are integers now, the calculation of  $\mathbf{q}_v^{(\ell+1)}$  requires only an integer multiplication, a RID or RIS and a clipping. Hence the requantization becomes integer-arithmetic-only.

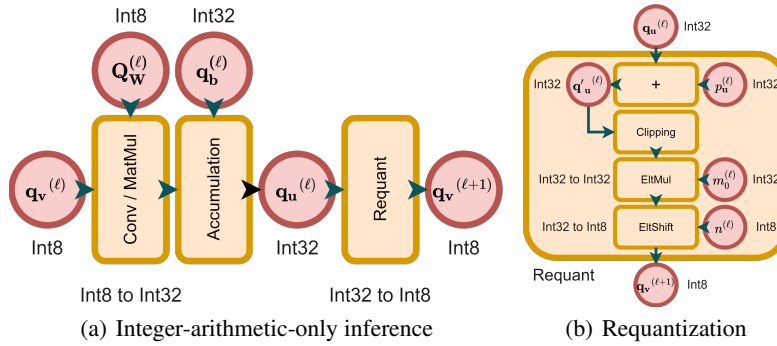


Figure 3: The integer-arithmetic-only inference. An offline-constrained integer-arithmetic-only re-quantization will be adopted during inference, which we will discuss in Section 3.2.

### 3 INTEGER-ONLY PTQ FOR DETERMINISTIC CODING

Different from works on general model quantization whose major purpose is to compress the model size and improve inference efficiency, we introduce quantization to eliminate the inconsistent arithmetic. Thus, we should strictly prevent using platform-specific operators. So we restrict all inference calculations to 32-bit integer arithmetic, as it is the most widely supported set of integer arithmetic by hardware devices. Particularly, leveraging execution efficiency and compatibility, we only consider adopting matrix multiplication on 8-bit integer operands to perform convolution.

#### 3.1 PTQ BASELINE

We adopt a relatively simple and standard quantization pipeline as described in Nagel et al. (2021). We apply symmetric per-channel quantization on weights and asymmetric per-tensor quantization on activation except the output of the last layer in parameter net. Instead, we symmetrically quantize the activation from the last layer to 16 bits, with a fixed quantization step  $2^{-6}$ . This benefits the CDF indexing and calculation which we will discuss later in Section 4.1. As recommended in Nagel et al. (2021), we adopt a grid search minimizing the reconstruction error to obtain the weight quantization step  $s_w$  of each layer. We figure out the activation quantization step  $s_u$  with Min-Max method on a little calibration data. After setting the quantizers, we apply a per-block (or per-network) adaptive rounding reconstruction (Brecq, Li et al. (2020)).

#### 3.2 OFFLINE-CONSTRAINED INTEGER-ARITHMETIC-ONLY REQUANTIZATION

Previous use of integer-arithmetic-only requantization is based on QAT (Jacob et al., 2018; Yao et al., 2021; Zhao et al., 2020). It is first proposed in Jacob et al. (2018) where  $m_0$  in eq. 4 is always set to an integer bigger than  $2^{30}$  which should be represented with 32 bits. We find it risky, as this 32-bit integer  $m_0$  will later multiply with the 32-bit integer accumulation. Assuming that no specific hardware support is available, we tend to believe that the requantization should be implemented with standard 32-bit integer arithmetic (*i.e.* we cannot conduct the bit-shift on 64-bit multiplication result registers). Thus, the 32-bit integer multiplication may overflow and result in error if we use unconstrained  $m_0$ . Another issue is, in Jacob et al. (2018) the requantization scale factor  $m$  is empirically assumed as always less than 1, which is hard to satisfy in PTQ.

To address this problem, we slightly modify the requantization by moving the zero-point adding operation in eq. 3 forward:

$$p_u^{(\ell)} = \left\lceil \frac{z_u^{(\ell)}}{m^{(\ell)}} \right\rceil \quad (6)$$

$$\mathbf{q}_v^{(\ell+1)} = \text{clip} \left( \left\lceil m^{(\ell)} \left( \mathbf{q}_u^{(\ell)} + p_u^{(\ell)} \right) \right\rceil \right) = \text{clip} \left( \left\lceil m^{(\ell)} \mathbf{q}'_u^{(\ell)} \right\rceil \right) \quad (7)$$

where  $\mathbf{q}'_{\mathbf{u}}^{(\ell)} = \mathbf{q}_{\mathbf{u}}^{(\ell)} + p_{\mathbf{u}}^{(\ell)}$  is the 32-bit integer activation biased with the 32-bit pre-scaling zero-point  $p_{\mathbf{u}}^{(\ell)}$ . By doing so, the asymmetric quantization of  $\mathbf{q}_{\mathbf{u}}$  changes to the symmetric quantization of  $\mathbf{q}'_{\mathbf{u}}$ . As the requantized value will be clipped to  $B$ -bit integer within a range  $[-2^{B-1}, 2^{B-1} - 1]$ , the maximal and minimal valid value of  $\mathbf{q}'_{\mathbf{u}}^{(\ell)}$  are computable:

$$q_{\max}^{(\ell)} = \left\lfloor \frac{2^{B-1} - 1}{m^{(\ell)}} \right\rfloor, \quad q_{\min}^{(\ell)} = \left\lceil \frac{-2^{B-1}}{m^{(\ell)}} \right\rceil \quad (8)$$

with these bounds, we can earlier conduct the clipping operation before the rescaling, restricting the biased activation values  $\mathbf{q}'_{\mathbf{u}}$  in the range  $[q_{\min}, q_{\max}]$ . Thus, we can figure out the largest  $n$  subject to  $\forall \mathbf{q}'_{\mathbf{u}} \in \mathbf{q}'_{\mathbf{u}}, -2^{31} \leq m_0 \mathbf{q}'_{\mathbf{u}} < 2^{31}$ , which avoids overflow while keeps precision as much as possible:

$$n^{(\ell)} = 32 - B, \quad m_0^{(\ell)} = \left\lfloor 2^{n^{(\ell)}} m^{(\ell)} \right\rfloor \quad (9)$$

Therefore, after setting the quantizers, we offline calculate the dyadic numbers and replace the re-quantization operations layer by layer. Empirically, the proposed integer-arithmetic-only re-quantization with constrained magnitude of  $m_0$  still keeps the model performance, though it introduces slightly more numerical error than the original version proposed in Jacob et al. (2018). We can safely adopt it across platforms with standard 32-bit integer multiplications and RISs/RIDs. Figure 3 (right) shows this offline-constrained form of re-quantization.

## 4 FROM 16-BIT OUTPUT TO DISCRETIZED CUMULATIVE DISTRIBUTION

### 4.1 BINARY LOGARITHM STD DISCRETIZATION FOR DETERMINISTIC ENTROPY MODELING

The network-output parameters should be discretized, so that the CDFs can be stored as limited look-up-tables (LUTs). In previously proposed approaches (Ballé et al., 2019; Sun et al., 2021), the standard deviations (STD) are logarithmically discretized with computing natural logarithm  $\log(\cdot)$ :

$$\hat{i}_{\sigma} = \left\lfloor \frac{\log(\sigma) - \log(\sigma_{\min})}{\Delta_{\sigma}} \right\rfloor \quad (10)$$

which is hard to determinize. Sun et al. (2021) obtains  $\hat{i}_{\sigma}$  from parameter network output in a deterministic way by comparing the fix-point  $\sigma$  value with pre-computed sampling points  $\hat{\sigma}$ . This is moderately efficient as there are 64 levels of  $\hat{\sigma}$  for each predicted STD to compare.

Empirically, the STD is long-tail distributed as most of the latents are predicted to have entropy close to zero. So the logarithmic discretization of  $\sigma$  is reasonable to suppress error and has been proved effective. To keep this favor and be more hardware-friendly, we propose to use binary logarithm. Hence, we modify eq. 10 to:

$$\begin{aligned} \Delta &= \frac{1}{L-1} \log_2 \left( \frac{\sigma_{\max}}{\sigma_{\min}} \right) \\ \hat{i}_{\sigma} &= \lfloor (\log_2(\sigma) - \log_2(\sigma_{\min})) \Delta^{-1} \rfloor \\ \hat{\sigma} &= \sigma_{\min} \left( \exp_2(\hat{i}) \right)^{\Delta} \end{aligned} \quad (11)$$

where  $\exp_2(x) = 2^x$  denotes the power of 2. Ballé et al. (2019) and Sun et al. (2021) adopt the same bounds  $\sigma_{\min} = 0.11$  and  $\sigma_{\max} = 256$  with level  $L = 64$ . To omit non-determinism while to simplify the calculation, we instead adopt  $\sigma_{\min} = 0.125$ ,  $\sigma_{\max} = 32$  and  $L = 9$ . Therefore, we obtain a simplified formula with  $\Delta = 1$  and  $\log_2(\sigma_{\min}) = -3$ . Since the STD has an extremely long-tail distribution, using a smaller upper bound  $\sigma_{\max}$  is painless. Adopting less levels, however, enlarges error because the sampling points get sparser. Thus, we uniformly interpolate additional 7 minor levels between each two adjacent major levels of  $\hat{\sigma}$ . Considering the input  $\sigma$  is the dequantized fix-point value with corresponding quantized integer  $q$  and scale  $s = 2^{-6}$  (i.e.  $\sigma = sq$ ), the updated

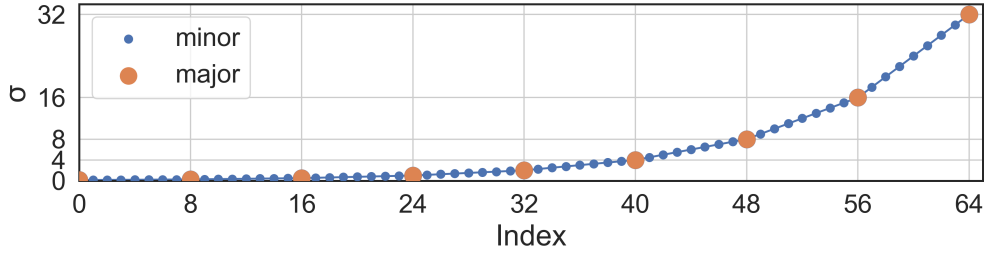


Figure 4: Visualization of the proposed 65-level STD parameter discretization. The orange dots denote binary-logarithmically distributed major levels and the blue ones are linearly interpolated minor levels.

formula is:

$$\begin{aligned}
\hat{i} &= \lfloor \log_2(q) \rfloor + \log_2(s) + 3 \\
\hat{j} &= \left\lfloor \frac{q - \exp2(\lfloor \log_2(q) \rfloor)}{\exp2(\lfloor \log_2(q) \rfloor - 3)} \right\rfloor \\
\hat{i}_\sigma &= 8\hat{i} + \hat{j} \\
\hat{\sigma} &= \sigma_{\min} \left( \exp2(\hat{i}) + \hat{j} \exp2(\hat{i} - 3) \right)
\end{aligned} \tag{12}$$

where  $\log_2(s) = -6$  is a constant integer.  $\hat{i} \in \{0, 1, \dots, 8\}$  and  $\hat{j} \in \{0, 1, \dots, 8\}$  are the major and minor indexes, respectively. Note that  $\hat{i} = 8$  iff.  $q = 2^{11}$ , when  $\hat{j} = 0$ . Thus, the summary index  $\hat{i}_\sigma \in \{0, 1, \dots, 64\}$  corresponds to 65 values of  $\hat{\sigma}$ , which generates 65 CDFs to be stored as LUTs. Figure 4 shows the value distribution of this discretization.

Thus, the calculation of  $\hat{i}_\sigma$  reduces to calculating the round-down integer binary logarithm of 16-bit integer  $q$ . To compute the binary-logarithm of an integer, we can adopt platform-specific instructions like BSR on x86 or CLZ on ARM. We can also use a platform-independent bit-wise algorithm to count the leading zeros to obtain result of integer binary logarithm, which is easy to vectorize.

#### 4.2 DETERMINISTIC ENTROPY CODING WITH GAUSSIAN MIXTURE MODEL

For models using GMM with  $k$  Gaussian components, we can calculate CDF of the  $i$ -th component with given  $\mu_i$  and  $\sigma_i$  and accumulate it with a multiplier  $\pi_i$ . The predicted multiplier is dequantized 16-bit fix-point number  $\pi_i = s_\pi q_{\pi_i}$ :

$$C_{\text{GMM}(\hat{y})}(\hat{y}; \pi, \mu, \sigma) = \sum_{i=1}^k s_\pi q_{\pi_i} C_{\hat{y}}(\hat{y}; \mu_i, \sigma_i) \tag{13}$$

where  $s_\pi$  is the quantization scale of  $q_{\pi_i}$ . We can omit  $s_\pi$  in eq. 13 because it is a constant scalar normalizer and can be merged into the normalization factor of frequency based CDF table. The remaining part only involves integer arithmetic.

To obtain the CDF of the  $i$ -th Gaussian component  $C_{\hat{y}}(\hat{y}; \mu_i, \sigma_i)$ , we can query two-level pre-computed LUTs with combined  $\hat{i}_\sigma$  (eq. 12) as outer index and  $\hat{y} - \lfloor \mu_i \rfloor$  in eq. ?? as inner index. However, indexing the inner level LUT with  $\hat{y} - \lfloor \mu_i \rfloor$  suffers from a risk of out-of-bound error. We cannot directly restrict the range of  $\hat{y}$  to  $[\lfloor \mu_i \rfloor - R, \lfloor \mu_i \rfloor + R]$  like Sun et al. (2021) because multiple Gaussian components are involved. If  $\exists \mu_j$  subject to  $\mu_i - \mu_j > R$ , the direct restriction may result in significant error. Instead, we set the cumulative distribution value to 0 and  $\text{CDF}_{\max}$  when  $\hat{y} - \lfloor \mu_i \rfloor \leq -R$  and  $\hat{y} - \lfloor \mu_i \rfloor \geq R$  respectively. We restrict the symbol  $\hat{y}$  no bigger than  $(\max \lfloor \mu \rfloor) + R$  where the CDF value is  $\text{CDF}_{\max}$ . Also we restrict it larger than  $(\min \lfloor \mu \rfloor) - R$  where the CDF value is zero. In situations the symbol  $\hat{y}$  is out of these upper and lower bounds, we will adopt Golomb coding to encode  $\hat{y}$ , inspired by tensorflow-compression implementation<sup>1</sup>. This

<sup>1</sup>[https://github.com/tensorflow/compression/blob/v2.2/tensorflow\\_compression/python/entropy\\_models/continuous\\_base.py#L80-L81](https://github.com/tensorflow/compression/blob/v2.2/tensorflow_compression/python/entropy_models/continuous_base.py#L80-L81)

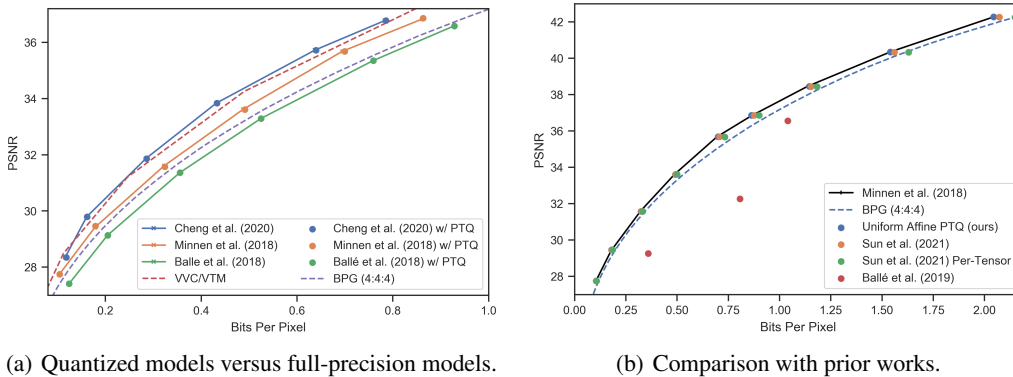


Figure 5: RD curves evaluated on Kodak. (a) RD performance of different models w/ or w/o quantization. The solid lines with cross markers denote original model inference with floating point numbers. The dots represent quantized 8-bit integer-arithmetic-only models, sharing the same color as its floating-point version. (b) We test Sun et al. (2021) by quantizing the activations in both per-channel and per-tensor manner. We also test Ballé et al. (2019).

situation is quite rare as its corresponding probability mass is close to zero, and adopting Golomb coding will not damage the overall bit rate. Thus, the CDF of GMM in eq. 13 is still monotonically increasing which can be reversed with searching algorithms during decoding.

With pre-computed CDFs of single mu-scale Gaussian entropy model, probability of  $\hat{y}_i$  in each Gaussian component can be checked from shared LUTs. Then the aggregated CDF value of  $\hat{y}_i$  can be calculated with given  $q_\pi$ .

## 5 EXPERIMENTS

We train various presently state-of-the-art learned image compression architectures on floating point to obtain the full-precision models. After the training, we use PTQ algorithms to quantize sub-networks involved in the entropy estimation to 8-bit, as above-mentioned. Then we replace all requantization and Leaky ReLU with corresponding deterministic adaptations and insert additional layers for LUT-index calculation.

### 5.1 COMPRESSION PERFORMANCE

Method	ours	Sun et al. (2021)	
Act. Quant.	per-tensor	per-channel	per-tensor
BD-Rate (%)	<b>0.35</b>	1.22	4.04

Table 1: BD-rates over full-precision model. The RD data is the same as that in Figure 5(b).

We quantize sub-networks of Ballé et al. (2018), Minnen et al. (2018), and Cheng et al. (2020) involving entropy prediction to 8-bit and compare their rate-distortion (RD) performance with original full-precision version, shown in Figure 5(a). The results indicate that, existing learned image compression techniques are compatible with standard PTQ. All tested models can infer with integer-arithmetic-only computations with negligible reduction on RD performance, which guarantees painless cross-platform consistency. It is not necessary any more for us to particularly develop new training techniques nor network structures to address the inconsistency issue.

We compare our approach with existing ones (Sun et al., 2021; Ballé et al., 2019). We present the RD results in Figure 5(b), and further report the corresponding BD-rates (Bjontegaard (2001)) in Table 1. When adopting our approach or Sun et al. (2021) on Minnen et al. (2018) model, the RD performance marginally deteriorates. However, Sun et al. (2021) adopts a per-channel activation quantization which is unfriendly to hardware implementation and rarely supported (Nagel et al.,



2021). When adopting Sun et al. (2021) with per-tensor activation quantization, the performance, especially at higher bit-rates, gets hurt significantly. We have successfully reproduced the good performance reported in Ballé et al. (2019) for determining Ballé et al. (2018) (not shown here), although we try hard, we find this method cannot keep marginal performance deterioration for determining context-model-involved architectures like Minnen et al. (2018). Note that Ballé et al. (2019) is a dedicated QAT method, we find it hard to train when applied on Minnen et al. (2018).

## 5.2 RATE OF DECODING ERROR

PTQ Encoding Platform	w/o PTQ (FP32)		w/ PTQ (Int8)	
	GPU	CPU	GPU	CPU
Error Rate on Kodak	12/24 (50.0%)	12/24 (50.0%)	<b>0/24 (0.0%)</b>	<b>0/24 (0.0%)</b>
Error Rate on Tecnick	72/100 (72.0%)	84/100 (84.0%)	<b>0/100 (0.0%)</b>	<b>0/100 (0.0%)</b>

Table 2: Decoding error rates of Minnen et al. (2018) when inference with or without PTQ. The results are tested on NVIDIA GTX 1060 (marked as *GPU*) and Intel Core i7-7700 (marked as *CPU*). The decoding is cross-evaluated on the two platforms, *i.e.* encoding on one and decoding on the other.

Following Ballé et al. (2019) and Sun et al. (2021), we report the rate of decoding error in Table 2 for completeness. As the networks have been strictly restricted to only perform 8-bit and 32-bit integer arithmetic, the inference is strictly deterministic.

## 5.3 LATENCY OF BINARY LOGARITHM BASED STD DISCRETIZATION

Method	Comparison (CompressAI)	Comparison (vectorized)	Calculation (ours)	Hyper Synthesis
Latency on Kodak	17.32	9.52	<b>4.35</b>	22.26
Latency on Tecnick	61.01	33.81	<b>9.48</b>	47.74

Table 3: Discretization latency with different approaches (unit: microsecond).

Table 3 shows the inference latency when adopting comparison-based discretization used by Sun et al. (2021) and our proposed calculation-based discretization. All the results are tested on NVIDIA GTX 1060. To evaluate the comparison-based approach, we refer to popular CompressAI (Bégaint et al., 2020) implementation<sup>2</sup> and also test another more efficient vectorized algorithm. The inference latency of hyper synthesis is also reported as a reference. The results on Kodak (resolution:  $512 \times 768$  px) prove that the directly calculated binary logarithm is more efficient, strongly suppressing the speed bottleneck of STD discretization. And the results on larger  $1200 \times 1200$  px Tecnick images indicate that this improvement can be more significant when compressing high-resolution images.

## 6 DISCUSSION

The mature investigation on general model quantization provides free lunch to us for establishing a cross-platform consistent entropy estimation approach, which is essential to practical learned image compression. In this paper, we experimentally prove that the non-consistency issue of state-of-the-art learned image compression architectures can reduce to an integer-arithmetic-only model quantization problem. With a standard PTQ scheme, we achieve deterministic compression models which have almost the same compression performance as their pre-quantized full-precision versions. This result is encouraging. Furthermore, we improve the parameter discretization and extend it to fit GMM entropy model. In the future, we will further delve into practical learned image compression by extending the rate-distortion tradeoff to rate-distortion-speed tradeoff.

<sup>2</sup>[https://github.com/InterDigitalInc/CompressAI/blob/v1.1.8/compressai/entropy\\_models/entropy\\_models.py#L653-L658](https://github.com/InterDigitalInc/CompressAI/blob/v1.1.8/compressai/entropy_models/entropy_models.py#L653-L658)

---

## REFERENCES

- Versatile video coding reference software version 11.0 (vtm-11.0), 2020. URL [https://vcgit.hhi.fraunhofer.de/jvet/VVCSsoftware\\_VTM/-/tags/VTM-11.0](https://vcgit.hhi.fraunhofer.de/jvet/VVCSsoftware_VTM/-/tags/VTM-11.0).
- Johannes Ballé, Valero Laparra, and Eero P Simoncelli. End-to-end optimized image compression. In *Int. Conf. on Learning Representations*, 2017.
- Johannes Ballé, David Minnen, Saurabh Singh, Sung Jin Hwang, and Nick Johnston. Variational image compression with a scale hyperprior. In *Int. Conf. on Learning Representations*, 2018.
- Johannes Ballé, Nick Johnston, and David Minnen. Integer networks for data compression with latent-variable models. In *Int. Conf. on Learning Representations*, 2019.
- Jean Bégaint, Fabien Racapé, Simon Feltman, and Akshay Pushparaja. Compressai: a pytorch library and evaluation platform for end-to-end compression research. *arXiv preprint arXiv:2011.03029*, 2020.
- Fabrice Bellard. Bpg image format, 2015. URL <https://bellard.org/bpg>.
- Yash Bhalgat, Jinwon Lee, Markus Nagel, Tijmen Blankevoort, and Nojun Kwak. Lsq+: Improving low-bit quantization through learnable offsets and better initialization. In *Proceedings of the IEEE/CVF Conference on Computer Vision and Pattern Recognition Workshops*, pp. 696–697, 2020.
- Gisle Bjontegaard. Calculation of average psnr differences between rd-curves. *VCEG-M33*, 2001.
- Zhengxue Cheng, Heming Sun, Masaru Takeuchi, and Jiro Katto. Learned image compression with discretized gaussian mixture likelihoods and attention modules. In *Proceedings of the IEEE/CVF Conference on Computer Vision and Pattern Recognition (CVPR)*, June 2020.
- Steven K Esser, Jeffrey L McKinstry, Deepika Bablani, Rathinakumar Appuswamy, and Dharmendra S Modha. Learned step size quantization. In *International Conference on Learning Representations*, 2019.
- Zongyu Guo, Zhizheng Zhang, Runsen Feng, and Zhibo Chen. Causal contextual prediction for learned image compression. *IEEE Transactions on Circuits and Systems for Video Technology*, 2021.
- Dailan He, Yaoyan Zheng, Baocheng Sun, Yan Wang, and Hongwei Qin. Checkerboard context model for efficient learned image compression. In *Proceedings of the IEEE/CVF Conference on Computer Vision and Pattern Recognition*, pp. 14771–14780, 2021.
- Benoit Jacob, Skirmantas Kligys, Bo Chen, Menglong Zhu, Matthew Tang, Andrew Howard, Hartwig Adam, and Dmitry Kalenichenko. Quantization and training of neural networks for efficient integer-arithmetic-only inference. In *Proceedings of the IEEE conference on computer vision and pattern recognition*, pp. 2704–2713, 2018.
- Raghuraman Krishnamoorthi. Quantizing deep convolutional networks for efficient inference: A whitepaper. *arXiv preprint arXiv:1806.08342*, 2018.
- Rundong Li, Yan Wang, Feng Liang, Hongwei Qin, Junjie Yan, and Rui Fan. Fully quantized network for object detection. In *Proceedings of the IEEE/CVF Conference on Computer Vision and Pattern Recognition*, pp. 2810–2819, 2019.
- Yuhang Li, Ruihao Gong, Xu Tan, Yang Yang, Peng Hu, Qi Zhang, Fengwei Yu, Wei Wang, and Shi Gu. Brecq: Pushing the limit of post-training quantization by block reconstruction. In *International Conference on Learning Representations*, 2020.
- G Martin. Range encoding: an algorithm for removing redundancy from a digitised message. In *Video and Data Recording Conference, Southampton, 1979*, pp. 24–27, 1979.
- David Minnen, Johannes Ballé, and George D Toderici. Joint autoregressive and hierarchical priors for learned image compression. In *Advances in Neural Information Processing Systems*, pp. 10771–10780, 2018.

- 
- Markus Nagel, Mart van Baalen, Tijmen Blankevoort, and Max Welling. Data-free quantization through weight equalization and bias correction. In *Proceedings of the IEEE/CVF International Conference on Computer Vision*, pp. 1325–1334, 2019.
- Markus Nagel, Rana Ali Amjad, Mart Van Baalen, Christos Louizos, and Tijmen Blankevoort. Up or down? adaptive rounding for post-training quantization. In *International Conference on Machine Learning*, pp. 7197–7206. PMLR, 2020.
- Markus Nagel, Marios Fournarakis, Rana Ali Amjad, Yelysei Bondarenko, Mart van Baalen, and Tijmen Blankevoort. A white paper on neural network quantization. *arXiv preprint arXiv:2106.08295*, 2021.
- Jorma Rissanen and Glen Langdon. Universal modeling and coding. *IEEE Transactions on Information Theory*, 27(1):12–23, 1981.
- Heming Sun, Lu Yu, and Jiro Katto. Learned image compression with fixed-point arithmetic. In *2021 Picture Coding Symposium (PCS)*, pp. 1–5. IEEE, 2021.
- Zhewei Yao, Zhen Dong, Zhangcheng Zheng, Amir Gholami, Jiali Yu, Eric Tan, Leyuan Wang, Qijing Huang, Yida Wang, Michael Mahoney, et al. Hawq-v3: Dyadic neural network quantization. In *International Conference on Machine Learning*, pp. 11875–11886. PMLR, 2021.
- Hengrui Zhao, Dong Liu, and Houqiang Li. Efficient integer-arithmetic-only convolutional neural networks. *arXiv preprint arXiv:2006.11735*, 2020.